

# Air-hole collapse and mode transitions in microstructured fiber photonic wires

E. C. Mägi, H. C. Nguyen and B. J. Eggleton

Centre for Ultrahigh-bandwidth Devices for Optical Systems (CUDOS), School of Physics  
University of Sydney, New South Wales 2006, Australia  
[egg@physics.usyd.edu.au](mailto:egg@physics.usyd.edu.au)

**Abstract:** We demonstrate robust, low bend loss photonic wires made from air-clad microstructured “grapefruit” fiber. By tapering the fiber and collapsing the air-holes, the guided mode evolves from being fully embedded within the fiber to a spatially-localized evanescent regime a few millimeters in length, where the mode is strongly influenced by the external environment. We show that in the embedded regime there is negligible loss when the taper is immersed in index-matching fluid, while in the evanescent regime the attenuation increases by over 35 dB. Furthermore, we show that an 11  $\mu\text{m}$  wire in the embedded regime can be bent to a radius as small as 95  $\mu\text{m}$  with bend-loss of 0.03 dB in a 500 nm band. The combination of spatial localization, strong dependence on the external environment and small bend radius make the device ideally suited for bio-photonic sensing.

©2005 Optical Society of America

OCIS codes: (060.2270) Fiber Characterization; (060.2310) Fiber Optics

---

## References and links

1. P. Russell, "Photonic crystal fibers," *Science* **299**, 358-362 (2003).
2. G.E. Town and J.T. Lizier, "Tapered holey fibers for spot-size and numerical-aperture conversion," *Opt. Lett.* **26**, 1042-1044 (2001).
3. J.K. Chandalia, B.J. Eggleton, R.S. Windeler, S.G. Kosinski, X. Liu, and C. Xu, "Adiabatic coupling in tapered air-silica microstructured optical fiber," *Photon. Tech. Lett.* **13**, 52-54 (2001).
4. S.G. Leon-Saval, T.A. Birks, W.J. Wadsworth, P.S.J. Russell, and M.W. Mason, "Supercontinuum generation in submicron fibre waveguides," *Opt. Express* **12**, 2864-2869 (2004).
5. M.A. Foster and A.L. Gaeta, "Ultra-low threshold supercontinuum generation in sub-wavelength waveguides," *Opt. Express* **12**, 3137-3143 (2004).
6. L.M. Tong, R.R. Gattass, J.B. Ashcom, S.L. He, J.Y. Lou, M.Y. Shen, I. Maxwell, and E. Mazur, "Subwavelength-diameter silica wires for low-loss optical wave guiding," *Nature* **426**, 816-819 (2003).
7. Y.K. Lize, E.C. Magi, V.G. Ta'eed, J.A. Bolger, P. Steinvurzel, and B.J. Eggleton, "Microstructured optical fiber photonic wires with subwavelength core diameter," *Opt. Express* **12**, 3209-3217 (2004).
8. M. Sumetsky, Y. Dulashko, and A. Hale, "Fabrication and study of bent and coiled free silica nanowires: Self-coupling microloop optical interferometer," *Opt. Express* **12**, 3521-3531 (2004).
9. OFS Laboratories, 600 Mountain Avenue, Murray Hill, NJ 07974 (2004).
10. T.A. Birks and Y.W. Li, "The Shape of Fiber Tapers," *J. Lightwave Technol.* **10**, 432-438 (1992).
11. K. Miyake, M. Hachiwaka, T. Kinoshita, S. Yamaguchi, H. Kubota, and S. Kawanishi. "Bend Resistant Photonic Crystal Fiber Compatible with conventional Single Mode Fiber." in *Proceedings of European Conference on Optical Communication*, ed. Stockholm, 2004), pp. Mo3.3.4.

---

## 1. Introduction

Microstructured optical fibers (MOFs) provide a novel waveguide platform for photonic devices offering new applications in telecommunications, metrology, sensing and bio-photonics [1]. The mode properties of these fibers can be further modified and enhanced through tapering of the fiber, modifying the mode properties [2], and engineering the nonlinearity and waveguide dispersion for Raman solitons [3] and supercontinuum generation

[4, 5]. Tapering also enables the fiber dimensions to be reduced to micron- and submicron-scales, potentially enabling photonic wires for photonic circuitry and sensing applications [6-8]. The ability to manipulate these photonic wires enables novel photonic structures, such as microcoil resonators [8].

Of significant interest are fibers that incorporate large air-holes in the cladding region, forming an inner-cladding region surrounding a Ge-doped core, where the core ensures efficient coupling to standard single mode fibers. These MOFs can be tapered down to micron-scales while retaining its cross-sectional structure [3]. In doing so, its waveguiding characteristics transition through distinct regimes: the *embedded* and *evanescent* regimes [7]. The first regime is encountered when the structural dimensions are larger than the wavelength scale. The fundamental mode is well confined within the fiber, due to the presence of the air-holes surrounding the core. The fiber in this case is therefore a robust optical waveguide, in which the core can resemble the nanowires reported by Tong *et al.* [6], but with the advantage of being protected from the external environment. Contrarily, the *evanescent* regime is encountered when the structural dimensions are comparable to or smaller than the wavelength scale. In this case, the mode no longer resolves the air-holes, and its field distribution extends beyond the fiber boundary. The resulting field is highly sensitive to the environment, making such a fiber particularly interesting for sensing applications.

In this paper, we demonstrate a photonic wire constructed by tapering a MOF, which possess a transition from an “embedded” regime in which the mode is confined within an inner cladding region, into an “evanescent” regime, through controlled collapse of the air-holes over a localized region. Instead of further shrinking the entire fiber, we post-process the tapered MOF in the waist region, where the mode is still embedded. This allows the mode to expand by removing the air-holes that act to confine the mode, essentially transforming the MOF into a solid rod of silica. By collapsing the air-holes gradually along a length of the tapered MOF, the expanded mode is able to contract back in to the core adiabatically with low loss, when the air-holes reappear further along the taper. In the embedded regime we demonstrate that these photonic wires can exhibit remarkably low bend loss. We demonstrate a taper in the *embedded* regime, with taper-loss below 0.2 dB which does not change when index-matched, and an equally low bend-loss at bend-radii as small as 95  $\mu\text{m}$ . We show that

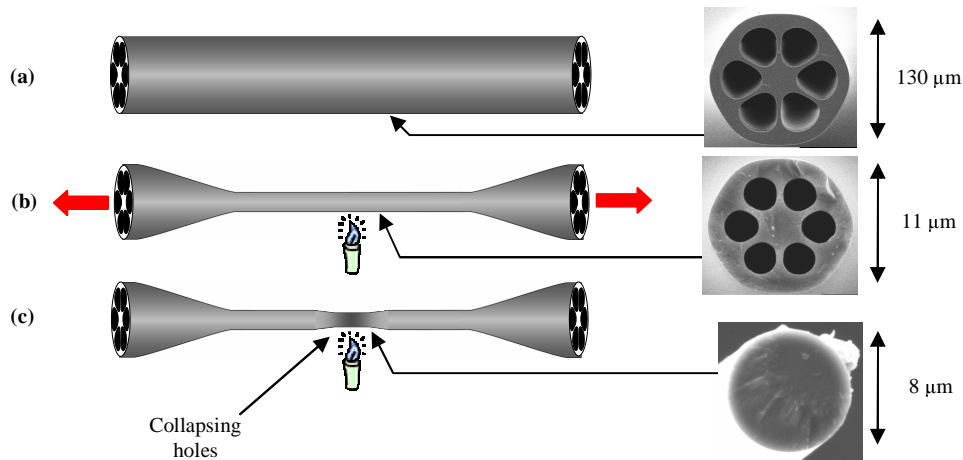


Fig. 1. Schematic of: (a) untapered MOF consisting of six air-holes surrounding a Ge-doped core; (b) the MOF tapered by stretching under a brushing flame, while maintaining the air-holes; (c) the local heat-treatment of the tapered MOF, where it is held stationary under a flame, causing the air-holes to collapse.

the air-holes can be collapsed over a localized few millimeter section of the taper, where the attenuation increases by more than 35 dB when index-matched.

## 2. Principle and fabrication

Figure 1 illustrates the tapered MOF geometry. The un-tapered MOF has an outer diameter of  $130\ \mu\text{m}$  and consists of six air-holes surrounding an inner-cladding region containing a Ge-doped core [3, 9]. The  $8\ \mu\text{m}$  doped core enables efficient, low-loss coupling to conventional single-mode fibers (SMFs), for in-situ transmission measurements. The MOF is adiabatically tapered down to a waist of  $11\ \mu\text{m}$  diameter and several centimeters in length, using a standard flame-brushing technique [10]. The cross-sectional structure is preserved by tapering “fast-and-cold” in which case the air-holes stay open and the mode remains confined and insensitive to the environment (Fig. 1(b)).

The waist of the taper is then post-processed by applying the flame without stretching the fiber (Fig. 1(c)). This localized heating allows the surface tension of the silica to collapse the holes over a small length of the taper, and as a consequence, further reduces the waist diameter to  $8\ \mu\text{m}$ . Scanning electron micrographs of sections of the MOF taper with and without the air-hole collapse are shown in Fig. 1.

Figure 2a illustrates the principle of the expanding mode through a simple simulation in beam-propagation method, using a  $6\ \mu\text{m}$  structure consisting of simplified circular air-holes. These simulations show the field intensity evolution of the fundamental mode at

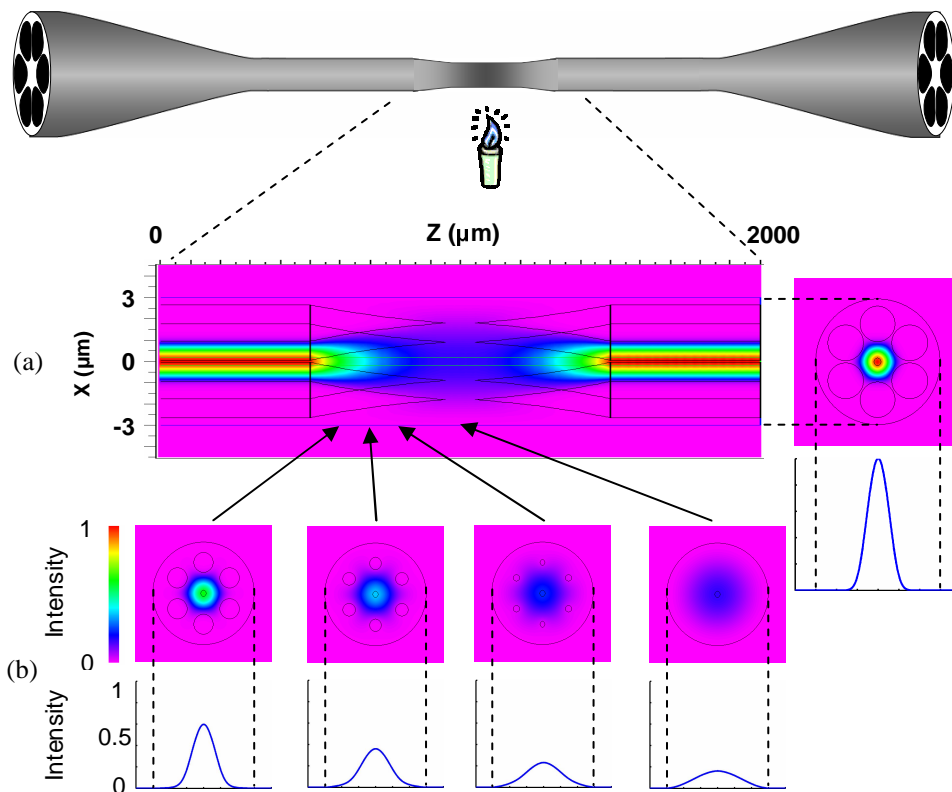


Fig. 2. (a) Simulated evolution of the field intensity as the core mode propagates through a region where the holes collapse and re-appear. The thin lines represent the outline of the taper and collapsing holes. The plot on the right shows the field intensity distribution of the launched mode. (b) Cross-sectional field intensity distribution at various positions along the taper, as the mode propagates through the heat-treated region.

$1.55\ \mu\text{m}$  wavelength, propagating through the  $2000\ \mu\text{m}$  length waist of tapered MOF, in which the air-holes collapse and re-appear. As the air-holes collapse, the initially-confined mode expands, eventually spanning the entire cross-section of the fiber and confined by the

outer silica-air boundary (Fig. 2(b)). When the holes disappear completely, a small portion of the field extends beyond the fiber boundary and becomes highly sensitive to the surrounding. At this diameter, the evanescent field is weak, and the propagation is strongly affected only when the taper is surrounded by index-matched fluid. We note that tapering the fiber to smaller dimensions would increase the evanescent field protruding outside the fiber. As the holes re-appear, the mode contracts and is confined in the core by the air-holes, eventually resembling the launched mode. The simulation yielded negligible loss from the propagation, indicating an adiabatic collapse and reappearance of the air-holes.

The air-holes of the MOF provide strong confinement that enables the mode to be fully embedded even at micron-scale diameters, where the mode density is low. This allows a short transition length over which the mode expands out to the evanescent regime adiabatically. In contrast, the low index contrast of SMFs results in the fundamental mode expanding through the cladding at a larger outer diameter. The higher mode density at these fiber dimensions require an SMF taper with a longer adiabatic transition length, in order for the fundamental mode to expand without coupling to other modes. In this respect, MOF photonic wires are advantageous not only in their small diameter while in the embedded regime, but also in the possibility of a more localized sensing region.

### 3. Measurement and discussion

Figure 3 shows three microscope images along the waist of a heat-treated taper. Figure 3(a) shows an image outside of the "heat-treated section" where the local waist diameter is 11  $\mu\text{m}$ . The presence of the air-holes is indicated by the horizontal lines running through the fiber. Figure 3(b) shows the transition region where the holes have collapsed partially, and Fig. 3(c) shows the waist region where the holes have collapsed completely, inferred from the lack of horizontal line structure within the image. This was confirmed by the SEM images shown in Fig. 1(c). The hole collapse transition occurred over millimeter length-scale.

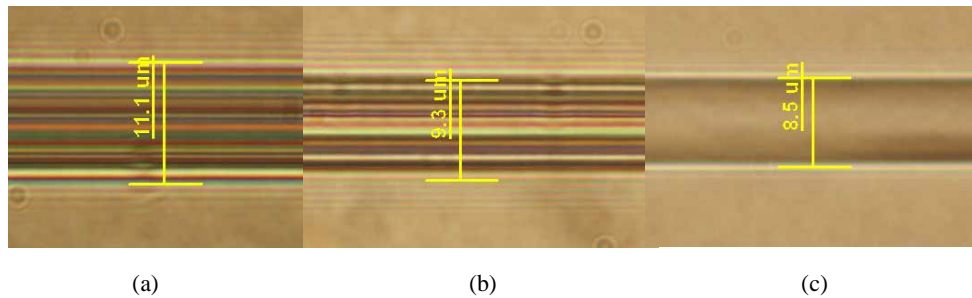


Fig. 3. Microscope images along an "adiabatic" heat treated Grape fruit fiber taper. (a) Outside of heat treated region (b) transition region where holes are collapsing, and (c) the waist where

The presence of the transition between the *embedded* and the *evanescent* regimes was determined by measuring the transmitted power and observing the change in the fiber sensitivity to the external environment. Figure 4 shows the transmission spectra of the tapered MOF, before and after heat-treatment, where the loss is below 0.1 dB before heat-treatment. When the taper is heat-treated so that the air-holes collapse, the loss remains under 1 dB, suggesting the mode re-adjusts itself as the holes re-appear further along the taper. Oscillations start to appear in the spectrum, indicating coupling to, and beating with, higher-order modes. Figure 4 also shows the spectra of the taper immersed in index-matching fluid, before and after heat-treatment. Prior to heat-treatment, the spectra of the taper with and

without index-matching overlay each other almost perfectly. This indicates strong confinement of the mode inside the fiber while the air-holes are open. On the other hand, when the heat-treated taper is index-matched, the transmitted power is strongly attenuated across the measured wavelength range of 1200 to 1700 nm, by more than 35 dB. The transmitted power for the index matched case is below the noise floor of the instrumentation. This is strong evidence that the collapse of the air-holes have allowed the mode to expand to the outer boundary of the fiber, becoming extremely sensitive to external disturbances.

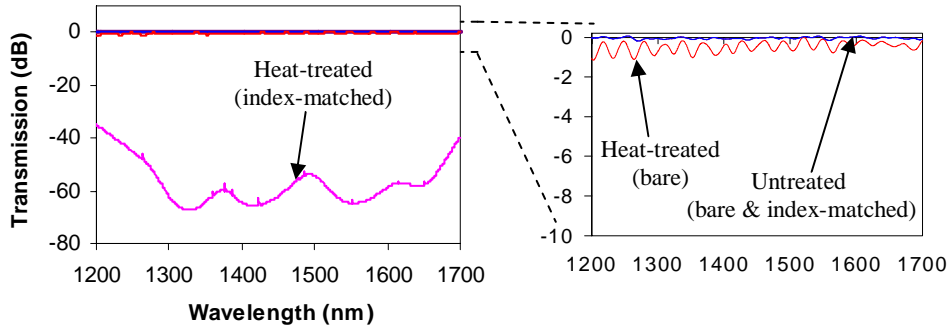


Fig. 4. Transmission spectra of tapered MOF relative to the untapered fiber. Prior to heat-treatment, the bare and index-matched tapers have identical spectra. After heat-treatment, when the holes have collapsed, the transmission in the index-matched case is lower by 40-70 dB.

The longitudinal variation in the fiber's sensitivity is mapped by scanning a small droplet of index-matching fluid, with a "wetted" diameter of approximately 300  $\mu\text{m}$ , along the heat-treated region of taper. This was achieved by attaching a small length of SMF-28 fiber to the flame nozzle of the taper rig and placing it in contact with the taper. A droplet of index-matching oil immersed both the SMF fiber and taper, surrounding their contact point, and this was scanned via a translation stage capable of 1  $\mu\text{m}$  position resolution. Figure 5 shows the longitudinal mapping of the attenuation due to the index-matching fluid, around the heat-

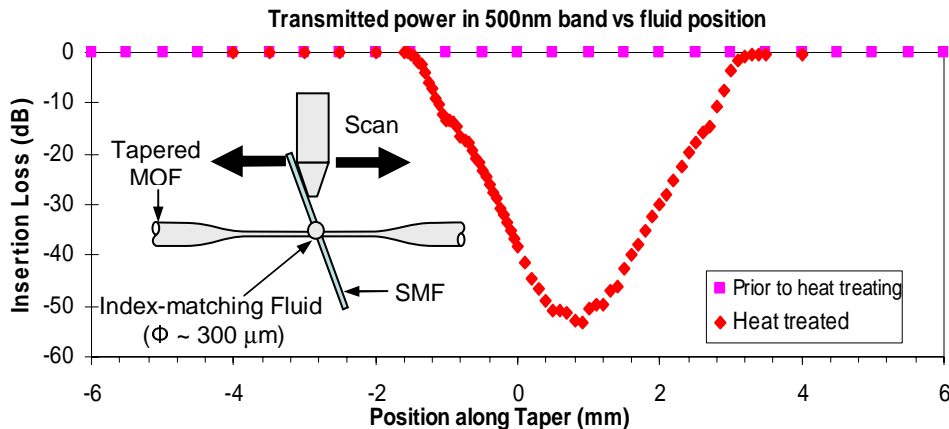


Fig. 5. Measurement of power transmitted through the taper, before and after heat-treatment, with an approximately 300  $\mu\text{m}$  droplet of index-matching fluid is applied at different positions along the taper. The schematic shows the fluid being applied using a SMF.

treated region of the taper. Negligible loss is observed prior to heat-treatment. Afterwards however, attenuation of up to 54 dB is observed, over a length-scale of approximately 5 mm, indicating that the mode expands and contracts adiabatically over this localized region. The

localization of this *evanescent* region is a great advantage for the tapered MOF geometry, particularly for applications in sensing.

Outside the heat-treated region, the presence of the air-holes provides strong confinement of light, resulting in low bend-loss. Figure 6 shows the bend-loss measurements for MOFs with 11  $\mu\text{m}$  diameter. The taper was wound into a loop by twisting one end by  $\sim 1.3$  revolutions. The twist was required to ensure the loop retained a planar geometry and a small length of acrylate coated SMF-28 fiber was inserted in the loop to act as a support. The bend radii were estimated via the position of the taper stages. The loop was tightened and only snapped when firmly wrapped around the acrylate coated fibre. The loss was measured to be below 0.01 dB in a 500 nm band, for bend-radii as small as 125  $\mu\text{m}$ . The fiber breaks at bend-radius of approximate 100  $\mu\text{m}$ , where the bend-loss begins to rise. Nevertheless, the loss observed here is significantly lower than those reported in Ref. [11] where almost 0.5 dB loss is observed per turn when an 80  $\mu\text{m}$  photonic crystal fiber is bent to a radius of 12 mm.

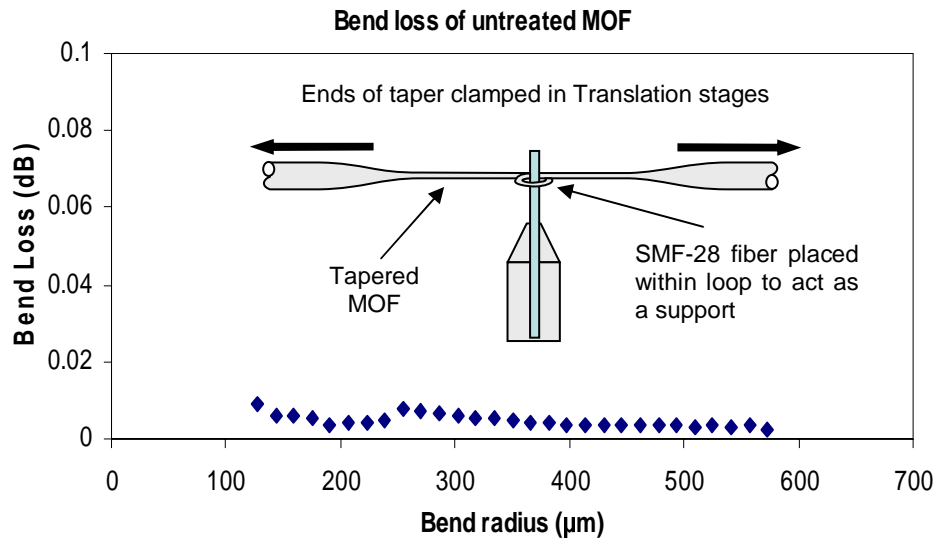


Fig. 6. Bend loss measurements of untreated MOF taper, in which the taper wound in a loop. Bend loss as a function of bend radius was measured in 500nm power band.

Figure 7 shows the spectral response for another 11  $\mu\text{m}$  diameter MOF wound around a stripped section of SMF-28 fiber with a bend radius of 95  $\mu\text{m}$ . The spectral response is measured in the range of 1200 nm to 1700 nm with a resolution of 5 nm. The bend-induced loss is just discernible for wavelengths above 1630 nm and the bend loss in a 500 nm band rises to 0.03 dB. The inset photograph in Fig. 7 shows a taper loop with minimum radius of curvature of 150  $\mu\text{m}$ . This was formed by twisting the taper by 5 revolutions. Power measurements on the loop showed no appreciable loss due to bending ( $< 0.03$  dB in 500 nm band) and no measurable coupling from the region of the taper waist which is in close contact. This clearly demonstrates the strong mode confinement within the core.

Such strong confinement enables the integration of the tapered MOF on to compact sensing devices, such as biological “lab on a chip”, where the taper could provide a robust, low-loss light delivery mechanism, while the heat-treated section would act as an efficient sensor. Furthermore, heat treatment should relieve bend induced stresses caused by looping the taper providing a more robust structure and thus allow unsupported permanent loops to be created.

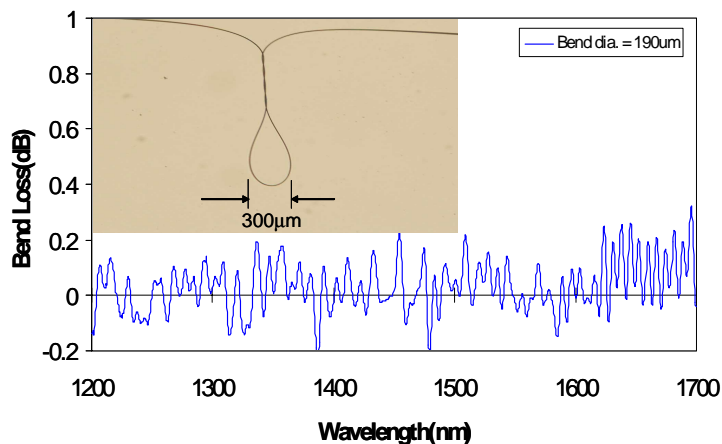


Fig. 7. Bend loss as a function of wavelength for bend radius of 95  $\mu\text{m}$ . Loss due to bending is just discernable for wavelength greater than 1630 nm.

#### 4. Conclusions

In this paper, we demonstrate the adiabatic transition and low bend loss of a tapered MOF and show that the mode field is confined within the inner cladding region and hence isolated from external environment. We further demonstrate that this taper can be post-processed by the application of heat, in order to collapse the air holes within a localized section of the taper. The mode field is then allowed to expand adiabatically to the surface of the taper thus exposing it to the external environment.

#### Acknowledgments

This work was produced with the assistance of the Australian Research Council under the ARC Centres of Excellence program. CUDOS (the Centre for Ultrahigh bandwidth Devices for Optical Systems) is an ARC Centre of Excellence.